

## Substituted Diketopyrrolopyrroles as Input Energy Units in Soluble Donor–Acceptor Dyads

Delphine Hablot,<sup>[a]</sup> Pascal Retailleau,<sup>[b]</sup> and Raymond Ziessel\*<sup>[a]</sup>

Diketopyrrolopyrroles (DPP) are highly colored pigments discovered about 35 years ago and characterized by their strong red color, extreme insolubility, and remarkable stability.<sup>[1,2]</sup> Many academic and industrial research development programs have since scrutinized the synthetic scope and spectroscopic potential of this interesting class of bicyclic lactams.<sup>[3,4]</sup> Of the many known pigments and dyes, DPP resembles a five-membered ring equivalent of epindolindione and quinacridone species, both of which find interesting applications after proper functionalization.<sup>[5]</sup> Given limitations in the availability of the starting materials, only a few means of preparing relatively soluble DPP dyes have been developed.<sup>[2–4]</sup>

In previous studies, we have demonstrated that the drawback of weak Stokes shifts of borondipyrromethene (BODIPY) dyes can be overcome by tethering polyaromatic fragments as energy input units.<sup>[6]</sup> Thus, due to very efficient intramolecular excitonic energy transfer (EET), large shifts (over 10000 cm<sup>-1</sup>) were routinely obtained.<sup>[7,8]</sup> Despite this advantage, due to the hydrophobic nature of pyrene and perylene substituents, the solubility in polar solvents was rather limited, prohibiting the use of such dyes under biological conditions. However, water-soluble BODIPY–fluorescein cassettes have recently been prepared as ratiometric pH reporters for imaging protein–dye conjugates in living cells.<sup>[9]</sup>

In light of the diverse spectroscopic properties of DPP and BODIPY dyes, it is tempting to link both kinds of dyes together to form soluble dyads in which the DPP moieties would serve as input energy absorbers under irradiation and favor EET to the BODIPY subunit. To the best of our knowledge, such combination has not been studied up to now. Many requirements have to be fulfilled to facilitate efficient fluorescence energy transfer and to avoid aggregation, although it may be noted that a DPP conjugated framework has been engineered to chelate boron and to promote near-infrared emission.<sup>[10]</sup>

As the first step towards the formation of a soluble derivative of DPP, we alkylated the bis-lactam **1** with benzylbromide using standard conditions<sup>[11,12]</sup> (Scheme 1); the intent being to inhibit the formation of hydrogen bonds and  $\pi$ – $\pi$  stacking responsible for the extreme insolubility of pigment **1**.

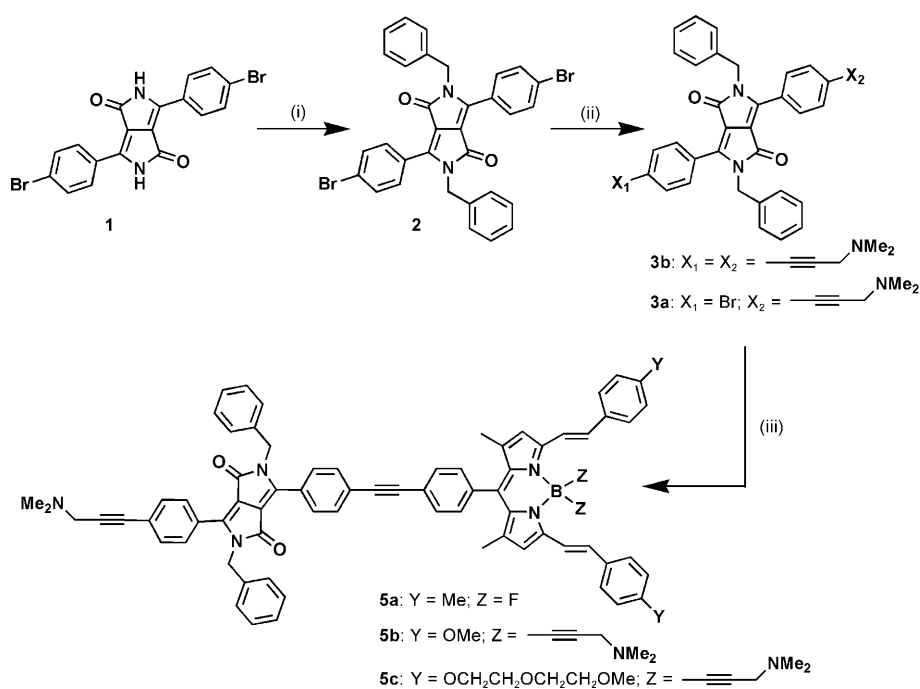
The X-ray crystal structure of the compound **2** has been determined (Figure 1). The molecule adopts a centrosymmetric conformation and is flanked by two solvent DMF molecules. Substitution around the pyrrolo[3,4–c]pyrrole ring results in some distorted bond lengths (e.g., C1–C11 1.439 Å vs. 1.481 Å usually observed) and angles (bond and torsional), as revealed by the program MOGUL.<sup>[13]</sup>

The antiparallel benzyl substituents on N1 and N1a are quasi-perpendicular to the central plane (making a dihedral angle of 89.7(2)°, whereas the lateral bromophenyl rings are twisted out of this plane by only 23.45(18)°. In the crystal, the molecules form infinite chains along the [1 –1 0] direction through paired C–Br... $\pi$ (benzyl at 1 + x, y – 1, z) orthogonal interactions 3.583(2) Å apart. The DPP platforms lie parallel to the (–2 –1 2) plane, generating intramolecular  $\pi$ – $\pi$  interactions between a bromophenyl ring at a general position and its symmetry-related one at (1–x, 1–y, 1–z), with an interplanar distance of 3.562(2), 1.255(2) Å of slip-page, and 3.010(2) Å long C–H(benzyl)... $\pi$  (phenyl–Br at –x, –y, 1–z) hydrogen bonds (Figure 2). In combination, these interactions result in a ladderlike substructure with benzyl groups and intercalated DMF molecules as lateral bars running along the [0 –1 1] direction (Figure S1 in the Supporting Information).

[a] D. Hablot, Dr. R. Ziessel  
Laboratoire de Chimie Moléculaire et Spectroscopies Avancées (LCOSA)  
Ecole Européenne de Chimie, Polymères et Matériaux  
CNRS, 25 rue Becquerel, 67087 Strasbourg Cedex 02 (France)  
Fax: (+33)3-90-24-26-89  
E-mail: ziessel@chimie.u-strasbg.fr  
Homepage: <http://www-lmspc.u-strasbg.fr/lcosa>

[b] Dr. P. Retailleau  
Laboratoire de Cristallographie, ICSN–CNRS  
Bât 27-1 avenue de la Terrasse  
91198 Gif-sur-Yvette Cedex (France)

Supporting information for this article is available on the WWW under <http://dx.doi.org/10.1002/chem.201001953>.



Scheme 1. i) Benzylbromide (10 equiv), DMF,  $\text{K}_2\text{CO}_3$  (11 equiv),  $120^\circ\text{C}$ , 2 h, 36%; ii) dimethylaminopropyne (1 equiv), benzene, triethylamine,  $[\text{Pd}(\text{PPh}_3)_2\text{Cl}_2]$  (10 mol%), CuI (15 mol%),  $40^\circ\text{C}$ , 60 h, 27% **3a**, 11% **3b**; iii) benzene, triethylamine,  $[\text{Pd}(\text{PPh}_3)_4]$  (10 mol%),  $50^\circ\text{C}$ , 15 h; 99% **4a** (1.2 equiv), 62% **4b** (1.0 equiv), 86% **4c** (1.0 equiv).

The next challenge in the synthesis consisted of chemical differentiation of both phenyl-Br groups by using an alkyne cross-coupling reaction promoted by palladium(0) and with dimethylaminopropyne as the substrate. The key tenet here was to introduce a polar function to easily separate the mono- and disubstituted derivatives by standard chromatog-

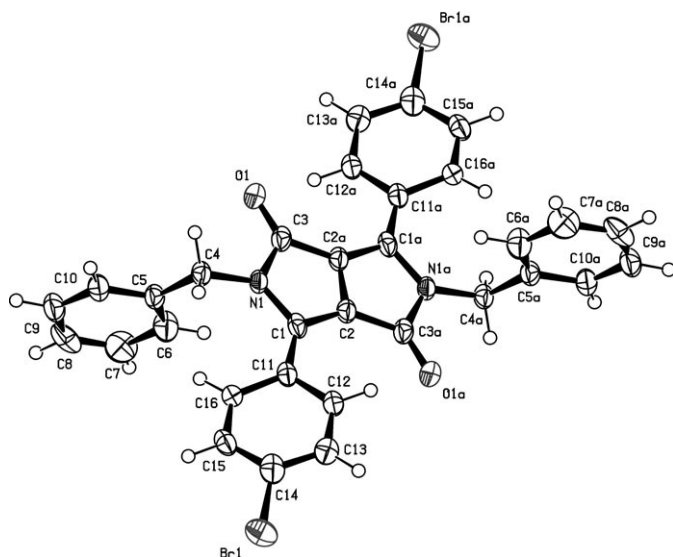


Figure 1. ORTEP view of the X-ray structure of compound **2**. Ellipsoids are drawn at the 50% probability level, H atoms as small spheres of arbitrary radii. The two solvent DMF molecules are omitted for clarity.

raphy. Cross-linking was effective, leading to dyes **3a** and **3b** depending upon the relative amounts of substrates (Scheme 1). The unreacted and less polar starting material **2** was easily recovered and recycled. Subsequently, two options were considered for coupling the blue BODIPY energy acceptors to the remaining phenyl-Br residue of compound **3a**. One was the attempted coupling of **3a** with trimethylsilylacetylene, followed by a deprotection step leading to the terminal alkyne ( $X_1 = \text{C}\equiv\text{CH}$ ,  $X_2 = \text{C}\equiv\text{CCH}_2\text{NMe}_2$  in **3**), but this failed due to the lack of reactivity of the terminal alkyne. Ultimately, the second option of post-functionalization of **3a** by using the stable BODIPY dyes **4a-c** pre-functionalized with the terminal alkyne was found to be successful. The cross-coupling was straightforward when using  $[\text{Pd}^0(\text{PPh}_3)_4]$  as the cata-

lyst precursor and triethylamine as the acid quencher. Average yields of about 50% were routinely obtained. Purification was facilitated by the polarity imported by the dimethylamino residues and/or the polyethyleneglycol side chains in the case of **4c**. All dual dyes were unambiguously characterized by NMR and FTIR spectroscopy, EI-MS and elemental analysis, and all data were consistent with their proposed molecular structures. The well-resolved NMR spectra confirmed the absence of aggregates and showed no clear indications of electronic perturbation of one substructure by another.

The electroactivity of the new dyes was measured by cyclic voltammetry and the data are gathered in Table 1. For **2**, a single oxidation peak was seen that could be ascribed to formation of the DPP  $\pi$ -radical cation. This peak was electrochemically reversible and corresponded to a one-electron process (Figure 3a). On reductive scans, two peaks were observed corresponding to reduction of DPP to its  $\pi$ -radical anion and dianion, respectively. The latter process was irreversible. As anticipated for **3a**, an additional irreversible oxidative peak attributed to the oxidation of the dimethylamino moiety was found at +1.11 V. The intensity of this wave at around +1.10 V increased in compounds **3b**, **4b**, and **4c** due to the increase of the number of dimethylamino substituents.

The anodic portion of the cyclic voltammogram recorded for **5a-c** was more complex than for the other compounds (Figure 3b). Based on the electrochemical properties recorded for **4a-c**, the first oxidation step was assigned to the

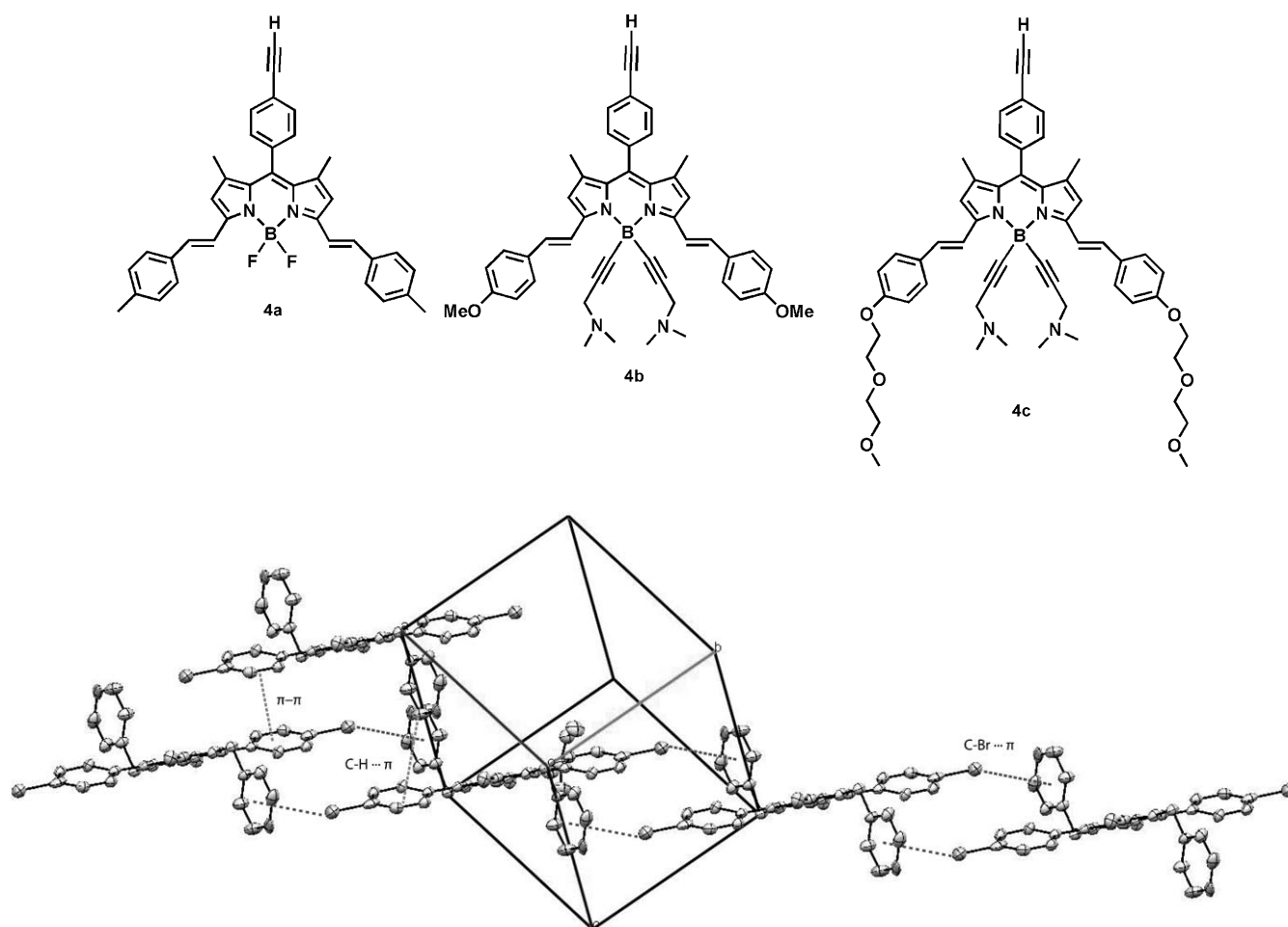


Figure 2. Part of the crystal structure of **2** showing the formation of a [1 -1 0] chain.

Table 1. Selected electrochemical data.<sup>[a]</sup>

	$E_{\text{ox}}^0$ , V ( $\Delta E$ [mV])		$E_{\text{red}}^0$ , V ( $\Delta E$ [mV])	
	DPP	BODIPY	DPP	BODIPY
<b>2</b>	+1.21 (60)	–	–1.14 (70); –1.86 (irr.)	–
<b>3a</b>	+1.22 (60), +1.11 (irr.) <sup>[b]</sup>	–	–1.15 (70); –1.82 (irr.)	–
<b>4a</b>	–	+0.82 (60), +1.35 (irr.) <sup>[c]</sup>	–	–0.96 (70); –1.80 (irr.)
<b>4b</b>	–	+0.76 (irr.), +1.12 (irr.) <sup>[b]</sup>	–	–1.14 (70)
<b>4c</b>	–	+0.66 (irr.), +1.10 (irr.) <sup>[b]</sup>	–	–1.16 (80)
<b>5a</b>	+1.29 (irr.)	+0.80 (irr.)	–1.10 (60); –1.72 (irr.)	–0.97 (60)
<b>5b</b>	+1.27 (irr.)	+0.74 (irr.)	–1.10 (60); –1.68 (irr.)	–1.15 (60)
<b>5c</b>	+1.27 (irr.)	+0.64 (irr.)	–1.14 (70); –1.74 (irr.)	–1.16 (70)

[a] Potentials determined by cyclic voltammetry in deoxygenated  $\text{CH}_2\text{Cl}_2$ , containing 0.1 M TBAPF<sub>6</sub>, at a solute concentration range of  $1.5 \times 10^{-3}$  M, at 20 °C. Potentials were standardized by using added ferrocene (Fc) as an internal reference and converted to SCE by assuming that  $E_{1/2}(\text{Fc}/\text{Fc}^+) = +0.38$  V ( $\Delta E_p = 70$  mV) versus SCE. Error in half-wave potentials is  $\pm 15$  mV. When the redox process is irreversible (irr.), the peak potential ( $E_{\text{ap}}$  or  $E_{\text{cp}}$ ) are quoted. [b] Corresponds to the irreversible oxidation of the tertiary amine. [c] Two-electron oxidation of the styryl/BODIPY subunit.

removal of one electron from the BODIPY unit. The additional broad irreversible wave at higher cathodic potential was assigned to overlapping of the oxidation of the DPP and dimethylamino residues. Interestingly, the DPP appendage in the dual dyes **5a–c** exerts no notable electronic effect on the overall electron donation and affinity of the BODIPY nucleus. These data indicate that the two partners DPP and BODIPY in **5a–c** are in weak electronic interaction, a situation generated by the twisted diphenylacetylene central linker as well as by the well-admitted orthogonality of the phenyl ring in the blue dyes **4a–c**. This latter situation is due to the presence of the bulky methyl groups in the 1,7-substitution position.<sup>[14]</sup>

Close examination of the spectroscopic properties reveals interesting features. Absorption spectra recorded for compounds **2**, **3a**, and **3b** in dioxane displayed features typical of the soluble DPP dyes, namely, a strong absorption in the visible region at around 480 nm. Along with other parent DPP dyes, the fluorescence spectra exhibited a maximum at around 550 nm with a shoulder at approximately 595 nm upon excitation at 446 nm (Figure 4a).<sup>[15]</sup> Since the intensity of the maximum band relative to the shoulder was independent of the concentration and nature of the solvent, it

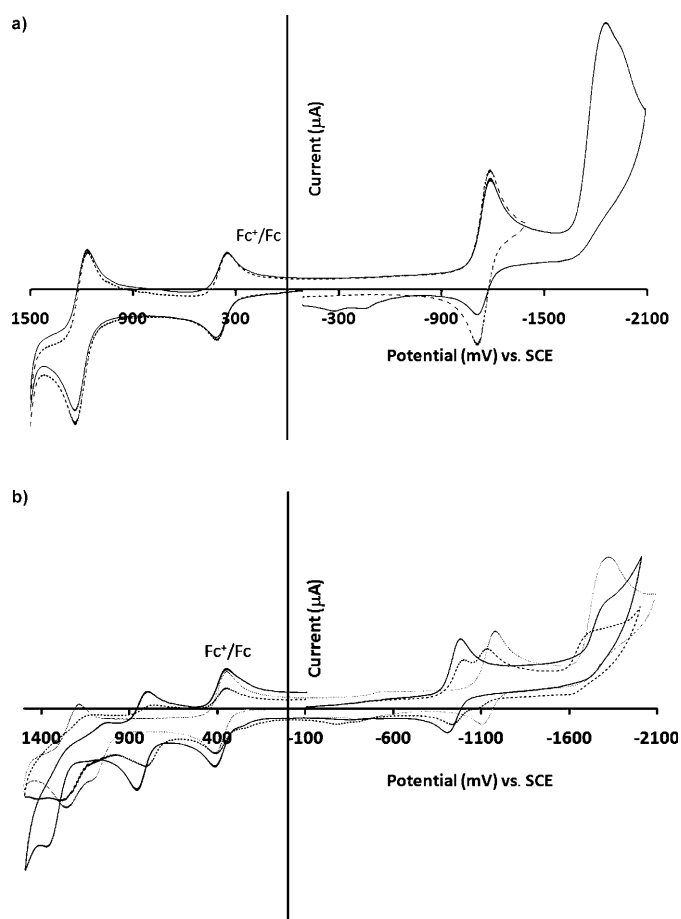


Figure 3. Cyclic voltammograms of a) **2** full window (plain line), limited to  $-1400$  mV (dashed line); b) **3a** (dotted line), **4a** (plain line), and **5a** (dashed line) in dichloromethane at RT. Fc corresponds to added ferrocene.

was concluded that this shoulder was not due to excimer emission. Quantum yields are gathered in Table 2 and the nanosecond excited-state lifetime regime is in keeping with a singlet excited state.

The absorption spectra of compounds **5a–c** is almost a linear combination of the absorption of the two separate

Table 2. Optical data measured at 298 K.

	$\lambda_{\text{abs}}$ [nm]	$\epsilon$ $\text{M}^{-1}\text{cm}^{-1}$	$\lambda_{\text{F}}^{\text{[a]}}$ [nm]	$\Phi_{\text{F}}^{\text{[b]}}$	$\tau_{\text{F}}$ [ns] $\pm 0.01$	$k_{\text{r}}^{\text{[c]}}$ $10^8 \text{s}^{-1}$	$k_{\text{nr}}^{\text{[c]}}$ $10^7 \text{s}^{-1}$
<b>3a</b>	483	19900	547	0.90	6.40	1.41	1.56
<b>3b</b>	488	23300	554	0.89	5.05	1.76	2.18
<b>5a</b>	496	27700	–	–	–	–	–
	633	117500	644	0.90	7.26	1.24	1.38
<b>5b</b>	495	29700	–	–	–	–	–
	644	119500	657	0.74	6.76	1.09	3.85
<b>5c</b>	494	33100	–	–	–	–	–
	644	127000	657	0.69	7.93	0.87	3.91

[a] By excitation at 480 nm. [b] Determined in dioxane ( $c \approx 1.10^{-6} \text{M}$ ) by using rhodamine 6G as a reference ( $\Phi_{\text{F}} = 0.78$  in water,  $\lambda_{\text{exc}} = 488 \text{nm}$ ).<sup>[16]</sup> All  $\Phi_{\text{F}}$  are corrected for changes in refractive index. [c] Calculated by using the following equations, assuming that the emitting state is produced with unit quantum efficiency:  $k_{\text{r}} = \Phi_{\text{F}}/\tau_{\text{F}}$ ,  $k_{\text{nr}} = (1 - \Phi_{\text{F}})/\tau_{\text{F}}$ .

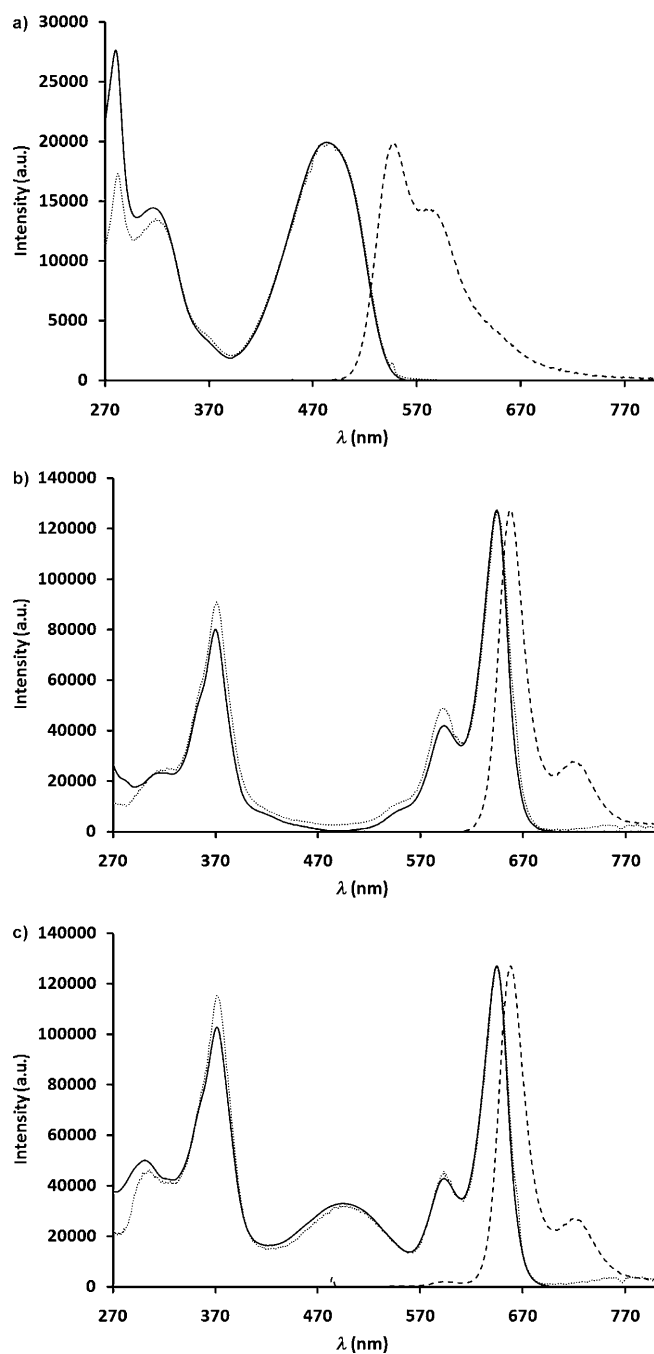
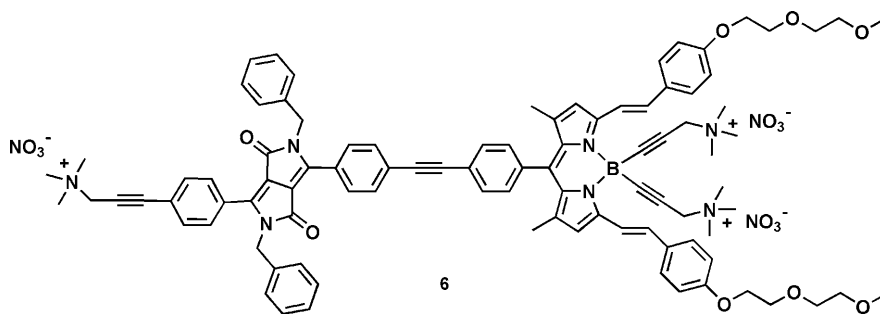


Figure 4. Absorption (—), emission (-----), and excitation (.....) spectra of a) dye **3a**, b) dye **4c**, and c) dual dye **5c** in dioxane at room temperature.

modules **3a** and **4a–c**, with a pronounced intramolecular charge transfer band (ICT) at 360 nm belonging to the blue part of the dual dye, a broad band characteristic of the DPP module, and the well-structured absorption of the  $S_0 \rightarrow S_1$  transition of the blue module at 650 nm (Figure 4c). In all three cases selective excitation in the DPP band at 470 nm revealed the absence of any residual DPP fluorescence and just the exclusive emission of the blue module at 660 nm. From the quantum yield determinations it appears that

quantitative energy transfer from the DPP to the blue dye occurs, excluding any determination of the residual excited-state lifetime. The rate of EET was estimated from our resolution limits to be very fast ( $>2 \times 10^{10} \text{ s}^{-1}$ ). Consistent with this result, the excitation spectra perfectly matched the absorption spectra over the entire spectral range (Figure 4c).

Interestingly, alkylation of **5c** with methyl iodide in anhydrous THF, followed by anion metathesis by using silver nitrate in methanol, afforded compound **6** in 92% yield. This form of **6** was highly soluble in methanol as well as in water/methanol mixtures, but unfortunately not in pure water.



The absorption spectra of **6** in methanol/water (80/20, v/v) showed similar features to those of **5c** and no significant aggregation was indicated by the absence of new absorption bands as commonly observed for BODIPY or DPP dyes (Figure 5).<sup>[17]</sup> Further, irradiation in the DPP subunit at 484 nm resulted in the exclusive emission from the blue dye unit at 644 nm as observed in apolar solvents. In this case, quantitative intramolecular energy transfer is also occurring (Figure 5a). We, however, noticed that quantum yield decreased from 19% in pure methanol to 12% with 5% water and to 9% with 20% water. This observation is not unusual and promoted by vibronic deactivation through the O–H bonds. We notice that, by increasing the water concentration to 20%, a weak residual emission of the DPP subunit is observed at 555 nm (Figure 5b). However, despite this weak decrease in intramolecular energy transfer, this result is auspicious for the use of such cassettes in biological conditions for multi-FRET (fluorescence resonant energy transfer) analysis.

In short, in this facile and straightforward route to soluble DPP-linked BODIPY dyes, the key step is the introduction of benzyl residues on the bicyclic lactam subunits. Differentiation of the two bromophenyl entities is feasible with a dimethylaminopropyne function, enabling the tethering of a blue BODIPY as an energy acceptor. Very weak interaction between the chromophores arising from the twisting of both phenyl fragments on the DPP side and the BODIPY sides, severely limits the electronic interactions between both photoactive modules. By excitation of the DPP module, a cascade energy transfer is effective with photons channeled to the blue dye, providing virtual Stoke shifts of about  $5610 \text{ cm}^{-1}$  (calculated by taking into account the energy dif-

ference between the input energy at 480 nm for DPP and the output energy at 657 nm for the blue BODIPY). The process is so efficient that no residual emission is observed, consistent with the operation of a Förster energy-transfer mechanism favored by the spectral overlap between the emission of DPP and the absorption of the blue dye. This discovery also holds true in polar solvents, including aqueous media. Further chemical modifications at the DPP are currently in progress to produce donor–acceptor systems suitable for incorporation in solar cells.<sup>[18]</sup>

## Experimental Section

### Selected data for compound **5a**:

<sup>1</sup>H NMR (300 MHz, CDCl<sub>3</sub>):  $\delta$  = 1.26 (s, 6H), 2.37 (s, 6H), 2.38 (s, 6H), 3.50 (s, 2H), 5.00 (s, 2H), 5.02 (s, 2H), 6.64 (s, 2H), 7.16–7.40 (m, 8 lines, 16H), 7.43–7.86 ppm (m, 14 lines, 18H);  
<sup>13</sup>C NMR (75.46 MHz, CDCl<sub>3</sub>):  $\delta$  = 15.0, 21.6, 29.8, 44.3, 45.9, 48.7, 85.0, 88.1, 90.3, 91.8, 110.2, 110.4, 118.0, 118.4, 123.7, 126.1, 126.6, 126.7, 126.8, 127.2, 127.7, 128.5, 128.7, 129.0, 129.1, 129.2, 129.7, 132.1, 132.2, 132.3, 132.5, 133.1, 133.9, 135.8, 136.6, 137.4, 137.6.

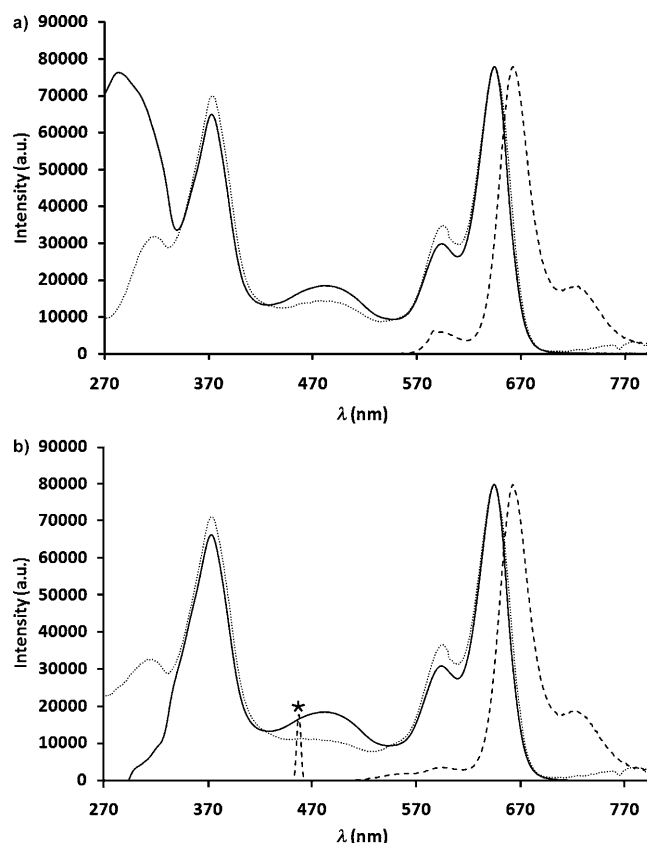


Figure 5. Absorption (—), emission (-----), and excitation (.....) spectra of: the tricationic dye **6** in a) methanol with 5% water, b) methanol with 20% water.

139.4, 141.8, 148.2, 148.6, 153.1, 162.8 ppm; ESI-MS ( $\text{CH}_2\text{Cl}_2 + 1\%$  TFA, +ve mode):  $m/z$  (%): 1100.3 (100); elemental analysis calcd (%) for  $\text{C}_{74}\text{H}_{60}\text{BF}_2\text{N}_5\text{O}_2$ : C 80.79, H 5.50, N 6.37; found: C 80.50, H 5.23, N 5.98.

**Compound 5b:**  $^1\text{H}$  NMR (300 MHz,  $\text{CDCl}_3$ ):  $\delta = 1.43$  (s, 6H), 2.20 (s, 12H), 2.36 (s, 6H), 3.22 (s, 4H), 3.49 (s, 2H), 3.86 (s, 6H), 5.00 (s, 2H), 5.02 (s, 2H), 6.64 (s, 2H), 6.93 (d,  $^3J = 8.6$  Hz, 4H), 7.08–7.41 (m, 10 lines, 14H), 7.45–7.85 (m, 12 lines, 14H), 8.23 ppm (d,  $^3J = 16.2$  Hz, 2H);  $^{13}\text{C}$  NMR (75.46 MHz,  $\text{CDCl}_3$ ):  $\delta = 15.2, 27.1, 44.1, 44.4, 45.9, 48.8, 49.9, 55.5, 84.9, 88.3, 90.3, 90.5, 92.1, 92.3, 110.2, 110.4, 114.4, 118.1, 119.6, 123.4, 126.2, 126.7, 126.8, 127.2, 127.7, 128.9, 129.0, 129.1, 129.2, 130.2, 131.4, 132.1, 132.2, 132.4, 133.9, 136.5, 137.4, 140.0, 148.3, 148.6, 152.2, 160.3, 162.8$  ppm; ESI-MS ( $\text{CH}_2\text{Cl}_2 + 1\%$  TFA, +ve mode):  $m/z$  (%): 1258.5 (100); elemental analysis calcd (%) for  $\text{C}_{84}\text{H}_{76}\text{BN}_7\text{O}_4$ : C 80.18, H 6.09, N 7.79; found: C 79.96, H 5.63, N 7.59.

**Compound 5c:**  $^1\text{H}$  NMR (400 MHz,  $\text{CDCl}_3$ ):  $\delta = 1.48$  (s, 6H), 2.19 (s, 12H), 2.36 (s, 6H), 3.21 (s, 4H), 3.41 (s, 6H), 3.49 (s, 2H), 3.57–3.63 (m, 4 lines, 4H), 3.72–3.77 (m, 4 lines, 4H), 3.90 (t,  $^3J = 4.6$  Hz, 4H), 4.20 (t,  $^3J = 4.6$  Hz, 4H), 5.00 (s, 2H), 5.02 (s, 2H), 6.64 (s, 2H), 6.94 (d,  $^3J = 9.2$  Hz, 4H), 7.08–7.41 (m, 11 lines, 14H), 7.46–7.84 (m, 11 lines, 14H), 8.22 ppm (d,  $^3J = 16.2$  Hz, 2H);  $^{13}\text{C}$  NMR (100.61 MHz,  $\text{CDCl}_3$ ):  $\delta = 15.2, 44.1, 44.4, 45.9, 48.8, 49.0, 59.3, 67.7, 69.9, 71.0, 72.1, 84.9, 88.6, 88.4, 90.2, 90.6, 92.0, 110.2, 110.4, 115.1, 118.1, 119.7, 123.4, 126.2, 126.8, 127.2, 127.7, 128.9, 129.0, 129.1, 129.2, 130.3, 131.4, 132.1, 132.2, 132.4, 133.9, 136.5, 137.4, 140.0, 148.3, 148.6, 152.2, 159.5, 162.8$  ppm; ESI-MS ( $\text{CH}_2\text{Cl}_2 + 1\%$  TFA, +ve mode):  $m/z$  (%): 1435.0 (100); elemental analysis calcd (%) for  $\text{C}_{92}\text{H}_{92}\text{BN}_7\text{O}_8$ : C 77.03, H 6.46, N 6.83; found: C 76.83, H 6.22, N 6.61.

**Compound 6:**  $^1\text{H}$  NMR (200 MHz,  $\text{CD}_3\text{OD} + \text{D}_2\text{O}$ ):  $\delta = 1.57$  (s, 6H), 3.09 (s, 18H), 3.27 (s, 9H), 3.44 (s, 6H), 3.57–3.69 (m, 4H), 3.78–3.92 (m, 4H), 3.85–4.03 (m, 4H), 4.23–4.42 (m, 4H), 4.47 (s, 4H), 4.78 (s, 2H), 5.17 (s, 4H), 6.99 (s, 2H), 7.15–7.76 (m, 10 lines, 18H), 7.87–8.99 (m, 8 lines, 14H), 8.34 ppm (d,  $^3J = 16.2$  Hz, 2H); ESI-MS ( $\text{CH}_2\text{Cl}_2 + 1\%$  TFA, +ve mode):  $m/z$  (%): 1602.6 (100), 513.6 (35); elemental analysis calcd (%) for  $\text{C}_{95}\text{H}_{101}\text{BN}_{10}\text{O}_{17}\cdot 2\text{H}_2\text{O}$ : C 66.89, H 6.44, N 8.21; found: C 66.79, H 6.04, N 8.07.

## Acknowledgements

We thank the Centre National de la Recherche Scientifique (CNRS) for financial support of this work and Professor Jack Harrowfield (ISIS in Strasbourg) for a critical reading of this manuscript prior to publication.

**Keywords:** diketopyrroles • dyes/pigments • energy transfer • pi conjugation • redox chemistry

- [1] D. G. Farnum, G. Mehta, G. G. Moore, F. P. Siegal, *Tetrahedron Lett.* **1974**, *15*, 2549–2552.
- [2] Z. Hao, A. Iqbal, *Chem. Soc. Rev.* **1997**, *26*, 203–213.
- [3] a) A. Iqbal, L. Cassar, US Patent 4,415,685, **1983**; b) J. Pfenninger, A. Iqbal, A. C. Rochat, Eur. Patent 184-981, **1986**; c) M. Jost, A. Iqbal, A. C. Rochat, Eur. Patent 224-445, **1987**.
- [4] A. Iqbal, M. Jost, R. Kirchmayr, J. Pfenninger, A. Rochat, O. Wallquist, *Bull. Soc. Chim. Belg.* **1988**, *97*, 615–643.
- [5] a) G. Lincke, *Dyes Pigm.* **2000**, *44*, 101–122; b) G. Lincke, *Dyes Pigm.* **2002**, *52*, 169–181.
- [6] A. Harriman, G. Izzet, R. Ziessel, *J. Am. Chem. Soc.* **2006**, *128*, 10868–10875.
- [7] a) G. Ulrich, R. Ziessel, A. Harriman, *Angew. Chem.* **2008**, *120*, 1202–1219; *Angew. Chem. Int. Ed.* **2008**, *47*, 1184–1201; b) A. Loudet, K. Burgess, *Chem. Rev.* **2007**, *107*, 4891–4932.
- [8] C. Goze, G. Ulrich, R. Ziessel, *J. Org. Chem.* **2007**, *72*, 313–322.
- [9] J. Han, A. Loudet, R. Barhoumi, R. Burghardt, K. Burgess, *J. Am. Chem. Soc.* **2009**, *131*, 1642–1643.
- [10] a) G. M. Fischer, A. P. Ehlers, A. Zumbusch, E. Daltrozzi, *Angew. Chem.* **2007**, *119*, 3824–3827; *Angew. Chem. Int. Ed.* **2007**, *46*, 3750–3753; b) G. M. Fischer, M. Isomäki-Kron Dahl, I. Göttker-Schnetmann, E. Daltrozzi, A. Zumbusch, *Chem. Eur. J.* **2009**, *15*, 4857–4864.
- [11] G. Colonna, T. Pilati, F. Rusconi, G. Zecchi, *Dyes Pigm.* **2007**, *75*, 125–129.
- [12] a) T. Yamagata, J. Kuwabara, T. Kanbara, *Tetrahedron Lett.* **2010**, *51*, 1596–1599; b) J. Kuwabara, T. Yamagata, T. Kanbara, *Tetrahedron* **2010**, *66*, 3736–3741.
- [13] I. J. Bruno, J. C. Cole, M. Kessler, J. Luo, W. D. S. Motherwell, L. H. Purkis, B. R. Smith, R. Taylor, R. I. Cooper, S. E. Harris, A. G. Orpen, *J. Chem. Inf. Comput. Sci.* **2004**, *44*, 2133–2144.
- [14] R. Ziessel, P. Retailleau, K. J. Elliott, A. Harriman, *Chem. Eur. J.* **2009**, *15*, 10369–10374.
- [15] a) L. Bürgi, M. Turbiez, R. Pfeiffer, F. Bienewald, H. Kimer, C. Winnewisser, *Adv. Mater.* **2008**, *20*, 2217–2224; b) A. B. Tamayo, B. Walker, T. Nguyen, *J. Phys. Chem. C* **2008**, *112*, 11545–11551; c) M. M. Wienk, M. Turbiez, J. Gilot, R. A. J. Janssen, *Adv. Mater.* **2008**, *20*, 2556–2560; d) K. Zhang, B. Tieke, *Macromolecules* **2008**, *41*, 7287–7295; e) D. Cao, Q. Liu, W. Zeng, S. Han, J. Peng, S. Z. Liu, *Macromolecules* **2006**, *39*, 8347–8355.
- [16] J. Olmsted, *J. Phys. Chem.* **1979**, *83*, 2581–2584.
- [17] a) I. Mikhalyov, N. Gretskaya, F. Bergström, L. B.-Å. Johansson, *Phys. Chem. Chem. Phys.* **2002**, *4*, 5663; b) D. Marushchak, S. Kalinin, I. Mikhalyov, N. Gretskaya, L. B.-Å. Johansson, *Spectrochim. Acta Part A* **2006**, *65*, 113–122.
- [18] L. Huo, J. Hou, H.-Y. Chen, S. Zhang, Y. Jiang, T. L. Chen, Y. Yang, *Macromolecules* **2009**, *42*, 6564–6571.

Received: July 9, 2010

Published online: October 29, 2010